Astronomy & Astrophysics

Accurate sticking coefficient calculation for carbonaceous dust growth through accretion and desorption in astrophysical environments

D. Bossion[1,2,★], A. Sarangi[3,4,★], S. Aalto[5], C. Esmerian[5], S. R. Hashemi[2], K. K. Knudsen[5], W. Vlemmings[5], and G. Nyman[2,★]

[1] Institute of Physics of Rennes, UMR-CNRS 6251, University of Rennes, 35000 Rennes, France
[2] Department of Chemistry and Molecular Biology, University of Gothenburg, 405 30, Gothenburg, Sweden
[3] DARK, Niels Bohr Institute, University of Copenhagen, Jagtvej 155A, 2200 Copenhagen, Denmark
[4] Indian Institute of Astrophysics, 100 Feet Rd, Koramangala, Bengaluru, Karnataka 560034, India
[5] Department of Space, Earth and Environment, Chalmers University of Technology, 412 96 Gothenburg, Sweden

ABSTRACT

Context. Cosmic dust is ubiquitous in astrophysical environments, where it significantly influences the chemistry and the spectra. Dust grains are likely to grow through the accretion of atoms and molecules from the gas-phase onto them. Despite their importance, only a few studies have computed the sticking coefficients for relevant temperatures and species, along with their direct impact on grain growth. Overall, the formation of dust and its growth are not well understood.
Aims. This study is aimed at calculating the sticking coefficients, binding energies, and grain growth rates over a broad range of temperatures, for various gas species interacting with carbonaceous dust grains.
Methods. We performed molecular dynamics simulations with a reactive force field algorithm to compute accurate sticking coefficients and obtain the binding energies. These results were used to build an astrophysical model of nucleation regions to study dust growth.
Results. We present, for the first time, the sticking coefficients of H, H_2, C, O, and CO on amorphous carbon structures for temperatures ranging from 50 K to 2250 K. In addition, we estimated the binding energies of H, C, and O in carbonaceous dust to calculate the thermal desorption rates. Combining accretion and desorption allows us to determine an effective accretion rate and sublimation temperature for carbonaceous dust.
Conclusions. We find that sticking coefficients can differ substantially from what is commonly used in astrophysical models. This offers us new insights into carbonaceous dust grain growth via accretion in dust-forming regions.

Key words. astrochemistry – accretion, accretion disks – molecular processes – methods: numerical – dust, extinction

1. Introduction

Dust grains in space provide a surface on which atoms and molecules may collide and stick, and also where they undergo chemical reactions. They are also important for the thermodynamics of the interstellar medium (ISM; Draine 2011). The evolution of dust grains in these processes depends on several factors, such as the physical conditions of the environment, the chemical type and morphology of the grains, and the abundance of the gas-phase species (Dwek & Scalo 1980; Tielens 1998; Dwek & Cherchneff 2011; Jones & Nuth 2011). When a species collides with a dust grain, its probability of sticking to the surface (and, hence, to participate to its growth by accretion) is called the sticking coefficient (Leitch-Devlin & Williams 1985; Laffon et al. 2021). This factor significantly impacts the evolution and processing of cosmic dust in astrophysical environments (Andersen et al. 2003), especially in regions where dust grains are thought to nucleate from the gas-phase in so-called nucleation regions: the winds of asymptotic giant branch (AGB) stars and the ejecta of core-collapse supernovae (CCSNe; Bocchio, Marco et al. 2014). Given a lack of theoretical predictions or experimental measurements, the previous literature has mainly treated the sticking coefficient as a parameter. In most cases, a fixed value has been chosen (e.g., 1 or 0.5, regardless of the type of gas particle) for the dust composition or the gas conditions (Dwek & Cherchneff 2011; Hirashita 2012). Here, we emphasize that the fate of cosmic dust largely depends on the sticking coefficients and requires a more accurate knowledge of such quantities.

Although the chemical and mineral composition of cosmic dust remains uncertain, both empirical constraints and theoretical considerations suggest that (especially in nucleation environments) cosmic dust consists mainly of two different species: carbonaceous and silicate dust (Tielens 2022). In O-rich nucleation environments, silicate dust is found and is composed of various species, but mainly O, Si, Fe, Mg, Ca, and Al (Henning 2010; Gobrecht et al. 2019), since most C is trapped in CO molecules. In C-rich nucleation environments, carbonaceous dust is formed and is composed mainly of C and H, with the O being trapped mostly in CO molecules. In this work, we are interested in the latter dust type.

★ Corresponding authors; duncan.bossion@univ-rennes.fr, sarangi@nbi.ku.dk, nyman@chem.gu.se

Due to the importance of accretion, which is the main grain growth mechanism along with coagulation, previous works have obtained sticking coefficients for some silicate and carbonaceous grains both theoretically (Leitch-Devlin & Williams 1985) and experimentally (Chaabouni et al. 2012). Concerning carbonaceous dust, calculations were carried out mainly on graphite-like surfaces (Leitch-Devlin & Williams 1985; Hollenbach & Salpeter 1970; Hollenbach & Salpeter 1971; Cazaux et al. 2011), which is one possible structure of carbon dust. However, spectroscopic evidence supports the notion that carbonaceous grains often take the form of amorphous carbon structures (Ehrenfreund & Cami 2010; Nashimoto et al. 2020; Cherchneff & Cau 1999), but the literature on sticking coefficients is sparse. Studies that do exist solely concern hydrogenated amorphous carbon (de Rooij et al. 2010; von Keudell et al. 2002) due to its importance in materials science. Many investigations also tend to focus on dust in cold environments (below 100 K), where the dust particles in circumstellar ejecta and nucleation environments can be partially coated with amorphous ice, for which more calculations and experiments are available (Buch & Zhang 1991; Masuda & Takahashi 1997; Al-Halabi et al. 2004; Chaabouni et al. 2012; Veeraghattam et al. 2014).

In the present work, we study the sticking process of different atomic and diatomic species on amorphous carbon particles. We compute the sticking coefficients as a function of temperature, ranging from 50 K to 2250 K, setting the dust and gas at the same temperature. In fact, this study provides sticking coefficients that are not available elsewhere in the literature and which are fundamental to model environments where carbon dust is present without an icy mantle and is in thermal equilibrium with the gas-phase; namely, primarily the circumstellar ejecta in which dust grains nucleate. Using these coefficients, we also show how the gas-phase chemistry will impact the growth of these grains.

In Sect. 2, we explain the numerical details and offer details on the amorphous carbon structure used and the dynamical calculations performed to determine sticking coefficients and binding energies. In Sect. 3, we present our results and a discussion, which includes the sticking coefficients we obtained, along with an application to the dust growth process in astrophysical environments. Finally, we give a discussion of the impact of this work and our conclusions in Sect. 4.

2. Numerical details

In this section, we describe the amorphous carbon grain used in our simulations. We also explain how the simulations were performed and how the binding energies were obtained.

2.1. Amorphous carbon structure

In this work, we focus on carbonaceous cosmic dust, which is mainly composed of amorphous carbon. Hence, this is the initial structure that we consider to compute the sticking coefficients. The structures used come from a library of tetrahedral amorphous carbon structures available in the literature (Deringer et al. 2018). These structures were obtained by combining molecular dynamics (MD) with a Gaussian approximation potential (GAP) based on machine learning (ML; Deringer & Csányi 2017). That ML-GAP procedure provides close-to-density functional theory (DFT) accuracy for a low computational cost. The authors created structures by taking slabs from an initial bulk obtained by GAP. They inserted a perturbation (by inserting a vacuum region) into those slabs. Then by MD, driven by ML-GAP, they

heated the surface from 300 K to 1000 K. This was followed by annealing at 1000 K and quenching at 300 K.

Here, we use their largest amorphous carbon structures, consisting of 512 carbon atoms, since our aim is to simulate atoms and diatomic molecules hitting a carbon dust structure composed of hundreds of atoms. We selected ten independent structures to obtain sticking coefficients averaged over those structures and obtain results that are as independent of the chosen amorphous carbon structures as possible and widely usable.

In order to use the described structures as carbonaceous dust, we first thermalized them to the temperature we are interested in, using a force field and a Nosé-Hoover chain (Nosé 1984; Hoover 1985). The sticking coefficient data are necessary for astrophysicists when carbonaceous dust is present. In dense environments in which dust grains form, at low temperature, below several tens of kelvins, an icy mantle forms around dust grains and changes the surface on which the incident particles hit. These mantles likely prevent the accretion of gas-phase atoms onto the solid dust substrate; therefore, we did not consider lower temperatures. Here, we chose to start at 50 K, where at least parts of the grains are not expected to have an icy mantle (Marchione et al. 2019; Potapov et al. 2020). Moreover, in most astrophysical models of environments that include dust, it is completely sublimated above 2000 K. Consequently, we focus on providing sticking coefficients in the 50–2250 K temperature range. In Fig. 1, we demonstrate how resilient these amorphous carbon structures are to temperature by thermalizing one structure at 50 K (panel A) and at 2500 K (panel B). At 50 K, the structure is similar to the original tetrahedral amorphous carbon structure, while at 2500 K, it loses its die shape and includes mostly two-dimensional (2D) cyclic units instead of three-dimensional (3D) bonds. This is due to the possibility of higher strength of bonds in cyclic compounds, making these shapes more resistant to high temperatures.

2.2. Dynamical calculation of sticking coefficients

This study is aimed at performing high-accuracy simulations of the dynamics of incident particles hitting carbon dust. Due to the high number of atoms present during the simulation (512 plus the incoming atoms), we chose to simulate the collisions using classical molecular dynamics. This approach is also consistent with the way the amorphous carbon structures were obtained. The movement of all the atoms and molecules is thus modeled using Newton's equations of motion, whereas all the forces are obtained based on force fields. To perform these simulations, we specifically used the reactive force field method (ReaxFF; van Duin et al. 2001), which allows for bond formation and bond breaking, which are expected to occur during atom sticking, together with the functional that was developed for hydrocarbon oxidation (Chenoweth et al. 2008) by the authors of this method. They optimized the parameters of this force field against quantum mechanical calculations. The latter were validated to yield an average error of 3.11 kcal.mol^{-1} for enthalpies of formation at 298 K. Our calculations were performed using the ReaxFF module of the Amsterdam Modeling Suite (AMS; van Duin et al. 2023), which is an optimization of the original ReaxFF code.

The environments in which cosmic dust is found include diffuse clouds (typically with densities up to 10^4 cm^{-3}; Potapov & McCoustra 2021). We can expect that each collision between an incident particle and the dust surface is independent of any earlier or later incoming particle. For this reason, we did not want the different incident particles to interact with each other during our simulation. Hence, for every simulation on a given

A

B
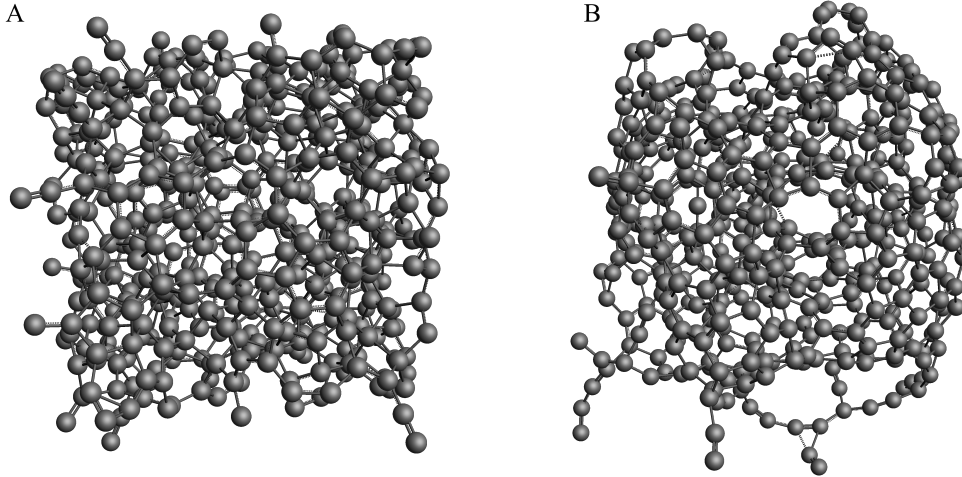
Fig. 1. Thermalized amorphous carbon structure. Panel A (left): at 50 K, presenting its original die shape, panel B (right): at 2500 K, presenting many two-dimensional cycles.

amorphous carbon structure, we launched colliding particles every 1250 fs and limit the investigation to only 37 particles in total to avoid the initial pure amorphous carbon structure from going too far from its original structure for all incident particles (it will contain at most 37 non-carbon atoms compared to the 512 carbon atoms in the cluster). To increase the statistics, we ran the simulation twice, leading to a total of 74 incident particles hitting each of the 10 amorphous carbon structures that we use, for a given temperature. Thus, each sticking coefficient is obtained based on a total of 740 collisions. It is important to note that this limits the accuracy of our sticking coefficients, as this prevents us from obtaining sticking coefficients of values lower than 10^{-3}. In addition, each incident particle is initially randomly placed in front of one of the six faces of the die-shaped amorphous carbon structure, at least 10 Å away from the closest carbon atom. This ensures that we maximize the number of amorphous carbon surfaces with which the incident particles will collide. The collision angle between the incident particles and the amorphous carbon structure is also randomly sampled.

To obtain the sticking coefficients corresponding to an environment at a given temperature, T, we initially thermalize the amorphous carbon structure. Although the initial velocity of the incident particle in a medium at temperature T is supposed to follow the Maxwell-Boltzmann velocity distribution, $f(v)$, it is important to note that colliding particles take a velocity-weighting factor as colliding particles with a high velocity collide more often than those with a low velocity. Hence, the velocity distribution that we consider in this work is

$$v f(v) = v \sqrt{\frac{2}{\pi}} \left(\frac{m}{k_B T}\right)^{3/2} v^2 \exp\left(-\frac{mv^2}{2k_B T}\right). \tag{1}$$

The AMS software does not allow us to directly sample velocities based on an arbitrary function, but only with Gaussian sampling, given a mean and a variance. The $v f(v)$ being already close to a Gaussian, we fit a Gaussian onto this distribution for each colliding particle and temperature and use the fitting parameters in our simulations. For incident diatomic molecules, we additionally give the individual atoms of the diatom an energy corresponding to the temperature T. This affects only its rotational and vibrational degrees of freedom. With this procedure, both the initial amorphous carbon structures and the incident particles are properly thermalized.

As the 512 carbon atom structures are not as large as carbonaceous dust particles (which can be as large as 0.1 μm in the

environments considered in this study), we also thermalized the amorphous carbon structure during the dynamics with a Nosé-Hoover chain every 100 fs. This ensures that the energy of the incident particles does not change the temperature of the amorphous carbonaceous dust grain, which is equivalent to having dust particles that are much larger than the incident particles or there being enough time between collisions to thermalize the structure. To ensure the best convergence of the chemisorbed and physisorbed rates, after the last incident particle is launched onto the surface, we extended the calculations for up to 0.45 ns. The sticking coefficient for chemisorption was obtained based on the results of the $n = 74$ incident particles hitting each of the $N = 10$ amorphous carbon structures, as follows:

$$P_\mathrm{x} = \frac{1}{N} \sum_{i=1}^{N} P_\mathrm{x}^{(i)} = \frac{1}{N} \sum_{i=1}^{N} \frac{N_\mathrm{x}^{(i)}}{n}, \tag{2}$$

where $P_\mathrm{x}^{(i)}$ is the sticking coefficient of the i-th structure for chemisorption (x≡chem) or physisorption (x≡phys), and $N_\mathrm{x}^{(i)}$ is the number of particles sticking to its surface through the process of interest, x. Thus, the sticking coefficient P_x is the mean of the distribution of $P_\mathrm{x}^{(i)}$. The error is computed as the variance of the mean sticking coefficients, obtained as

$$\sigma_{P_\mathrm{x}}^2 = \frac{1}{N} \sigma_{P_\mathrm{x}^{(i)}}^2 = \frac{1}{N} \left(\frac{1}{N} \sum_{i=1}^{N} (P_\mathrm{x}^{(i)} - P_\mathrm{x})^2 \right), \tag{3}$$

with $\sigma_{P_\mathrm{x}^{(i)}}$ the variance of the distribution of $P_\mathrm{x}^{(i)}$. The results presented in Sect. 3 are of the form $P_\mathrm{x} \pm \sigma_{P_\mathrm{x}}$.

2.3. Binding energy estimations

We are interested in estimating the binding energies of the C, O, and H atoms on the amorphous carbon structure. To do this, we used the energies calculated during the dynamics obtained through the simulations using ReaxFF (i.e., obtained with a force field). We first obtained the binding energy of C atoms, E_d^C, by considering the energy of a whole amorphous carbon structure thermalized at any temperature (the binding energy is temperature independent), divided by the number of C atoms in the structure, N^C. We note that during the thermalization of the structure, some C atoms might desorb and, hence. $N^\mathrm{C} \leq 512$. For the other species X (X≡C or X≡H), we considered the total
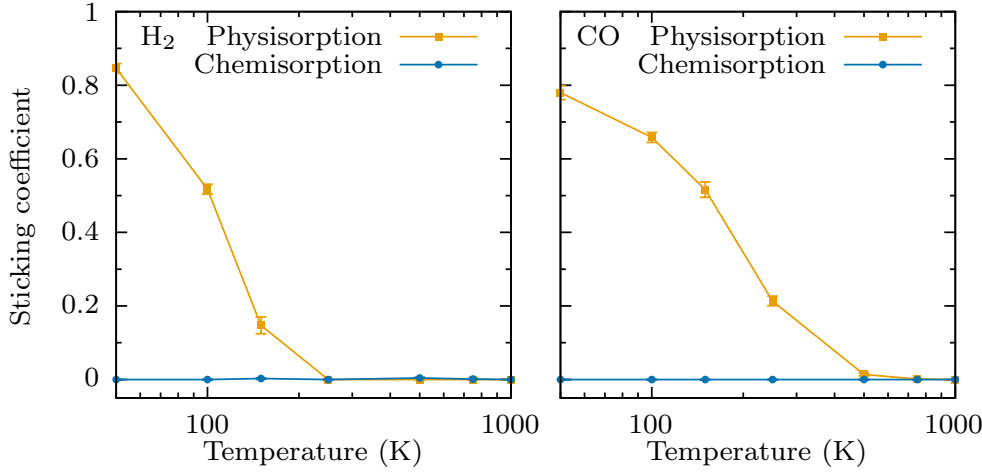
Fig. 2. Sticking coefficients as a function of temperature. Temperature ranging from 50 to 1000 K, for H_2 (left panel) and CO (right panel) on an amorphous carbon structure.

energy of the structure, including the chemisorbed X atoms at the end of a simulation, when the structure is fully thermalized. From this, we removed the energy coming from the C atoms and divided by the number of X atoms chemisorbed on the surface considered, as

$$E_d^C = \frac{E_d^{tot}}{N^C}; \qquad E_d^X = \frac{(E_d^{tot} - N^C E_d^C)}{N^X}. \qquad (4)$$

To ensure our results are independent of the choice of the structure and increase their accuracy, we reproduced this calculation for nine different amorphous carbon structures, at nine different temperatures. The error was computed as the variance of the mean value, similarly to Eq. (3).

3. Results and discussion

Here, we present the calculated sticking coefficients and binding energies we obtained to estimate a desorption rate. We conclude the work in this section by applying these sticking coefficients and binding energies to estimate dust growth rates in relevant astrophysical environments.

3.1. Sticking coefficients

We present the sticking coefficients of various colliders onto amorphous carbon structures. The results include physisorption, where the Van der Waals interactions allow the collider to move around on the amorphous carbon structure without creating a chemical bond and chemisorption for which the creation of a valence bond between the collider and the amorphous carbon structure allows the latter to grow by accretion. The physisorbed atoms, which are only present below about 250 K, can eventually desorb from the surface, on a much longer timescale at low temperature than at high temperature, with timescales of the order of nanoseconds down to a few picoseconds. The results belong to either of two groups: the non-reactive or the reactive colliders.

In the non-reactive group, no chemisorption is observed and the colliders are only physisorbed. Hence, these colliders cannot participate in the growth of cosmic dust. We found that among the colliders we consider in this study, H_2 and CO (presented, respectively, in the left and right panels of Fig. 2) are non-reactive colliders, as they cannot easily create covalent bonds with the surface. We do not observe any breaking of H_2, as the dissociation energy of its bond is above 400 kJ.mol^{-1} (48 110 K), or of CO, which was expected since it is the strongest known
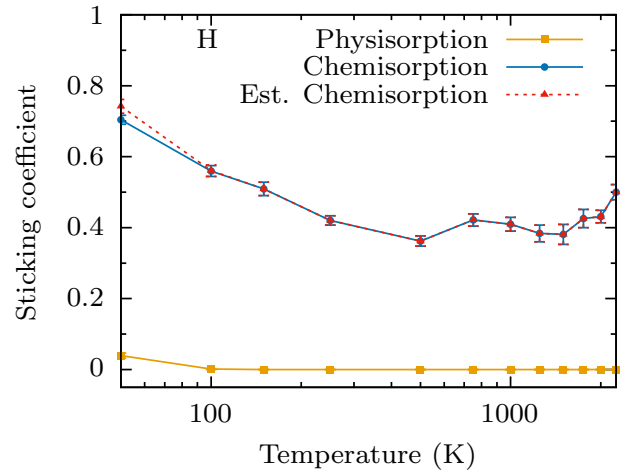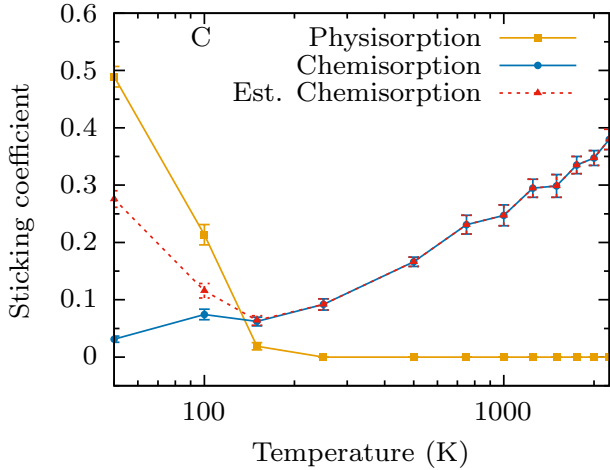

Fig. 3. Sticking coefficients as a function of temperature. Temperature ranging from 50 to 2250 K for H on an amorphous carbon structure.

diatomic bond, with a dissociation energy of over 1000 kJ.mol^{-1} (120 270 K). For those two colliders, we present the sticking coefficients for physisorption over temperatures from 50 K to 1000 K. It is important to note that these coefficients are time-dependent, as the physisorbed H_2 and CO molecules will desorb after a given temperature-dependent time (longer for lower temperatures). Physisorption is restricted to temperatures of up to 600 K, as only Van der Waals forces bind the physisorbed species to the surface.

When H, C, or O is the collider, there is a possible sticking through chemisorption. These colliders hence actively participate in the growth of carbonaceous cosmic dust through collision followed by accretion. For those colliders, both chemisorption and physisorption can happen. For dust growth, only chemisorption will have significance. Hence, for low temperatures, where the coefficient for sticking by physisorption is very high, we estimate a temperature-dependent rate for the conversion from physisorption to either desorption or chemisorption, which yields an estimated long-time chemisorption.

Figure 3 presents the temperature-dependent sticking coefficient of H on amorphous carbon. This coefficient is very high, particularly at low temperature, as it almost reaches 0.75 at 50 K. As the temperature increases, it quickly decreases to plateau around 0.4, and starts increasing again over 1500 K. It is interesting to note that over the 750–1500 K temperature range,

Fig. 4. Sticking coefficients as a function of temperature. Temperature ranging from 50 to 2250 K for C on an amorphous carbon structure.
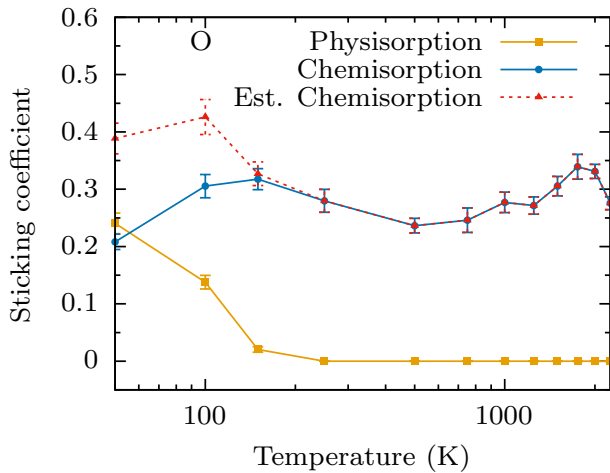
Fig. 5. Sticking coefficients as a function of temperature. Temperature ranging from 50 to 2250 K for O on an amorphous carbon structure.

the sticking coefficient appears to be temperature-independent. There is almost no physisorption even at 50 K, as the atomic hydrogen creates valence bonds very efficiently and, thus, rapidly chemisorbs.

The C and O sticking coefficients on the amorphous carbon are presented in Figs. 4 and 5, respectively. The profiles of the H, C, and O sticking coefficients over temperature are very different qualitatively and quantitatively, emphasizing the importance of direct dynamical calculations compared to rough estimates. When solely considering the initial chemisorbing fraction of C, we can see that it is clearly increasing with the temperature over the whole range considered, going from an almost non-reactive behavior at 50 K to a sticking coefficient of about 0.38 at 2250 K. On the other hand, the chemisorption rate of O is almost temperature independent, oscillating between 0.25 and 0.35 over the whole 50 K to 2250 K temperature range, with a slight decrease below 100 K. At low temperatures (from 50 K to 250 K), we observe both chemisorption and physisorption.

We want to estimate a sticking coefficient including only chemisorption and no physisorption, considering that cosmic dust is in media diffuse enough that all physisorbed atoms will eventually chemisorb or desorb before being directly involved in another collision with a collider. This is confirmed in the left panel of Fig. 6, which presents an estimated desorption rate (of physisorbed atoms) for C and O atoms. It is clear that physisorbed particles are not expected to play a role in the growth of carbon dust because they remain physisorbed on a much shorter timescale ($\ll 1$ s^{-1}) than the average collision time.

We investigated how many of the physisorbed colliders will eventually desorb and how many will chemisorb. The ambient conditions do not change over the time scale during which this occurs. It happens in less than a few nanoseconds; hence, all parameters remain unchanged. We find it a good approximation to observe what happens during 0.45 ns and compute the coefficients on that basis to estimate the long-time result. In the right panel of Fig. 6, we present the probability that initially physisorbed atoms chemisorb onto the surface, P_{PtC}. This probability is much higher for O atoms than for C atoms, and decreases with temperature, remaining relatively constant over 150 K. We note that the 50 K data point for O atoms is based on very low statistics and is therefore not as reliable as the other data presented. Similarly, there were not enough physisorbed H atoms to compute the probability over 100 K.

Based on P_{PtC}, and on the sticking coefficient for chemisorption, P_{chem}, and for physisorption, P_{phys}, we can estimate the final sticking probability of chemisorption, $P_{\text{chem}}^{\text{est}}$, for H, C, and O atoms on amorphous carbon; in this case, all the atoms are chemisorbed or desorbed, without the need to perform numerically expensive calculations to converge those coefficients until the point where all physisorbed atoms desorb or chemisorb. The estimated chemisorption sticking coefficients (represented with dashed red lines in Figs. 3, 4 and 5) are obtained as:

$$P_{\text{chem}}^{\text{est}} = P_{\text{chem}} + P_{\text{phys}} \times P_{\text{PtC}}. \tag{5}$$

The results at low temperature are drastically changed when the long-term behavior is considered, namely, when all physisorbed atoms have either been chemisorbed or desorbed. The physisorbed O atoms are efficiently chemisorbed, given enough time, and many C atoms are first physisorbed at low temperatures, even if those are less efficiently chemisorbed afterward. This leads the estimated sticking coefficient for the chemisorption of C at 50 K to jump from 0.03 to 0.28, while that of O jumps from 0.2 to almost 0.4. The estimated chemisorption sticking coefficient is higher for O atoms than for C atoms on the 50 K-to-1000 K temperature range. Those coefficients are about equal between 1000 K and 2000 K and the sticking of C atoms is more efficient than the sticking of O atoms above 2000 K, where the coefficient for the O atoms starts decreasing. This is an important result, as it shows that once the carbonaceous dust seed is created, O atoms will stick to it for most temperatures more likely than C atoms, thereby changing the pure amorphous carbon structures over time to structures that include both C and O atoms in an environment where they are both present. However, carbonaceous dust forms mostly in the ejecta of C-rich stars rather than O-rich stars, so this effect will be reduced in these conditions because most O atoms will be trapped in CO molecules, which are non-reactive on carbonaceous dust grains. It is interesting to note that the sticking coefficient of O atoms is nearly temperature-independent over 150 K, while this is not the case for C atoms, for which sticking values steadily increase with the temperature over 150 K.
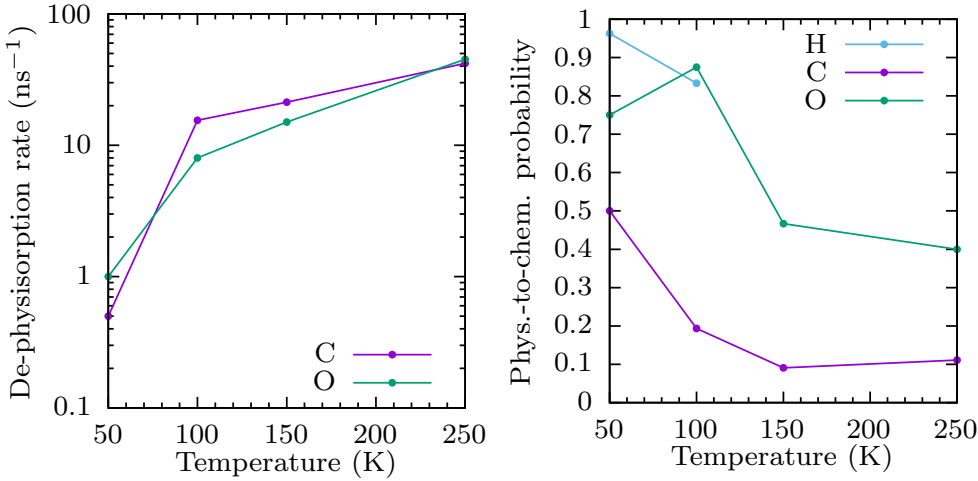
Fig. 6. Temperature-dependent quantities related to accretion. Left panel: temperature-dependent de-physisorption rate of the C and O atoms from the amorphous carbon structure. Right panel: probability that physisorbed H, C, and O atoms chemisorb onto the amorphous carbon structure as a function of temperature.

Table 1. Binding energies. Computed for H, C, and O with C atoms of the amorphous carbon structure.

Species X	H	C	O
Binding energy E_d^X (eV)	4.76 ± 0.12	7.55 ± 0.01	7.68 ± 0.21

To make the results presented in this work accessible and usable, they are all given in Table A.1 along with their uncertainties.

3.2. Binding energies

To study the growth rate of amorphous carbon dust, we need to account for the thermal desorption of initially chemisorbed atoms, which depends on the temperature and the binding energy of the desorbing species. In this work, we estimate the binding energies that we need using a force field, as detailed in the Sect. 2. Binding energies are presented in Table 1, where carbon and oxygen atoms have larger binding energies than hydrogen atoms due to their ability to not only form single bonds. The binding energy for the C atom is consistent with results found in the literature, where binding energies of C atoms on graphene were found to be around 7–8 eV (Oli et al. 2013). It can be noted that those values correspond to average binding energies, while some atoms might have higher or lower binding energies, depending on the number of bonds formed with the dust grain and on the local structure of the grain around the binding region. It can be expected that the more weakly adsorbed species will desorb preferentially. The binding energies we computed here may therefore be a slight overestimate for the purposes of calculating thermal desorption rates.

3.3. Application to dust growth

In stellar ejecta where dust grains form, molecules and dust form through nucleation and condensation of gas-phase atoms (Sarangi et al. 2018). Amorphous carbon or graphite dust is known to form in regions where the C/O ratio is typically greater than 1 (Fabbian et al. 2009), for example in the He-shell of core-collapse supernovae (Sarangi et al. 2018; Sarangi 2022) or the winds of C-rich AGB stars (Nanni et al. 2019; Marini et al. 2021). In such environments we expect to find atoms and molecules such as C, O, H, CO, He, H_2, CO_2, CH, and so on. In this paper,

we explore the probability that several of these species (i.e., H, H_2, C, O and CO) stick to the surface of a given dust grain.

For a grain of radius a, the rate at which it will accrete a particular gas-phase species on its surface depends on (a) its geometric cross-section, (b) the velocity of the incoming gas-phase species (which depends on the gas temperature T_g), (c) the density of that species in the gas, and also (d) the efficiency of sticking on the surface, which is commonly called the sticking coefficient. This accretion coefficient is defined as the rate of sticking F_i of a given species i (see Eq. (6)), as a function of the dust grain radius a and temperature, T_d, and the density of species n_i (Dwek & Cherchneff 2011; Hirashita 2012).

$$F_i(a, n_i, T_d, T_g, t) = \pi a^2 S_i(T_d, T_g) n_i(t) v_i^{th}(T_g), \quad (6)$$

where $S_i(T_d, T_g)$ is the temperature-dependent sticking coefficient of gas species at temperature, T_g, on a dust grain at temperature, T_d, and $v_i^{th}(T_g)$ is the thermal velocity of the species, i, here at the same temperature, $T_d = T_g = T$, as the dust grain. Combining the accretion rate of all species in the gas-phase, the rate at which the mass of a dust grain $m(a, t)$ will change is therefore given by

$$\frac{dm(a, t)}{dt} = \sum_i m_i F_i, \quad (7)$$

with m_i being the mass of species i. When atoms or molecules accrete on the surface of the dust grains, their abundances in the gas drop at the same rate (Hirashita & Kuo 2011). If we assume a general time-dependence of the gas density (without accretion) in a given environment as $n \sim t^p$, then after accretion on the dust-surface, the remaining species of type i in the gas is given by

$$n_i(t + \Delta t) = (n_i(t) - n_d(t) F_i \Delta t) \left(1 + \frac{\Delta t}{t}\right)^p, \quad (8)$$

where $n_d(t)$ is the number density of dust grains in the gas, since each of those grains will accrete at the same rate. In any freely expanding gas, such as stellar winds or explosions, the power law exponent p is given by -3.

In parallel to accretion, the dust grains also undergo desorption of atoms from their surface because the atoms may leave the grains when they gain enough energy to overcome the binding energy. The D_i rate for the desorption of species i strongly
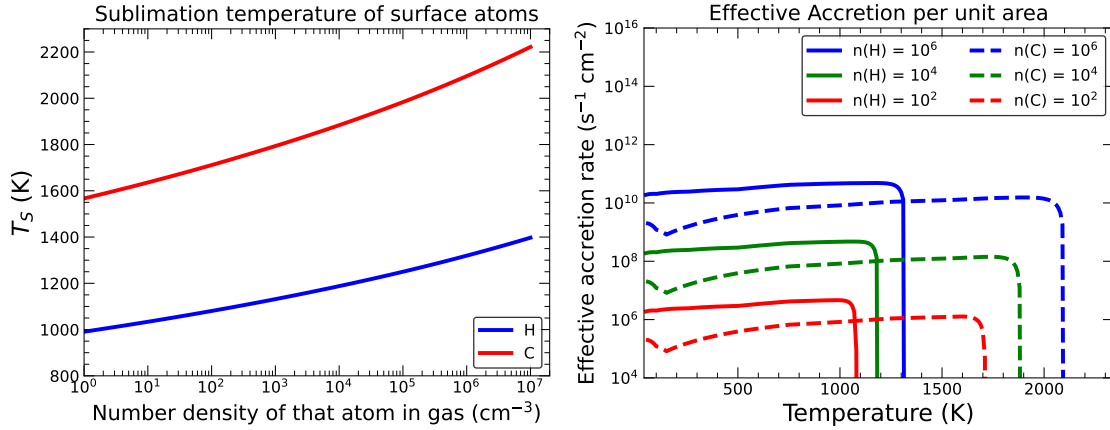
Fig. 7. Carbonaceous dust growth. Left panel: sublimation temperature, where the accretion and desorption rates on the surface of amorphous carbonaceous dust grains balance each other out, shown as a function of densities of C and H atoms in the gas. Right panel: effective accretion rates as a function of temperature on the surface of amorphous carbonaceous dust grains (effective number of accreting atoms per unit time per unit area), shown for different densities of C and H atoms in the gas. This is therefore the grain growth rate for the given conditions.

depends on the dust temperature and can be expressed by the Polanyi-Wigner equation ([Potapov et al. 2018](#)) as

$$D_i(a, T_d, t) = \Lambda_i(a)\, \nu_i\, e^{(-E_d^i/k_B T_d)}, \tag{9}$$

where, Λ_i is the number of surface atoms, ν_i is the attempted frequency for escape, E_d^i is the binding energy of species i, and k_B is the Boltzmann constant. Comparing the rate of accretion to that of desorption, we find the temperature where these two rates are equal to be

$$F_i(a, n_i, T_S, T_g, t) = D_i(a, T_S), \tag{10}$$

which represents the sublimation temperature, T_S. In the conditions considered here, the temperature of the gas and dust is the same, hence, $T_g = T_S$. Above this temperature, the grains rapidly lose atoms and sublimate.

In circumstellar environments, where carbonaceous dust can form, C, H, He, O, CO, and H_2 are often abundant. When the C/O ratio is larger than 1, there are almost no O atoms left in the gas by the time the smallest grains of carbonaceous dust are formed. The O atoms are trapped in CO molecules ([Cherchneff 2000](#); [Cherchneff et al. 2000](#); [Sarangi et al. 2018](#)). As Fig. 2 clearly indicates, the efficiency of CO and H_2 sticking on a surface of amorphous carbonaceous dust is almost negligible. The efficiencies of sticking of H and C atoms are shown in Figs. 3 and 4, respectively.

For the frequency, ν_i, in the desorption rate (see Eq. (9)), we use the vibrational frequency of the C–C and C–H bonds as 3×10^{13} and 9×10^{13} s^{-1}, respectively ([Stuart 2004](#)). Since both accretion and desorption rates have the same dependency on the surface area of the dust grains, the sublimation temperature, T_S, is thus independent of the grain size. In Fig. 7 (left panel), the sublimation temperature is shown for the C and H atoms on our amorphous carbonaceous dust grains as a function of their respective density in the gas-phase. The C atom has a higher sublimation temperature given its larger binding energy.

As the density of atoms drop in the gas, the sublimation temperature declines, since there are fewer atoms in the gas to accrete on the surface that can balance the desorption process. We call the difference between the accretion and the desorption rate the effective accretion rate. Figure 7 (right panel) presents the effective accretion rate of C and H atoms for different densities, based on the individual sticking coefficients calculated in

this study. As shown above (and consistently with the figure), the efficiency of H-sticking on our amorphous carbonaceous dust grains is greater than that of C-sticking, the difference being more pronounced at lower temperatures. More importantly, at higher temperatures, the H atoms desorb much faster than the C atoms. Therefore, in a cooling gas, like most stellar winds or ejecta, the initial phase of the grain growth will be dominated by dust made purely from C atoms, and C atoms will get depleted in the gas through sticking on the surface of the grains. As the gas further cools, the H atoms, based on how abundant H is, will start accreting on the surface of the grains, rapidly forming new hydrocarbons and possibly polyaromatic hydrocarbons (PAHs). It is important to note that a fraction of H is also bound in molecular H_2, which has a very low sticking probability. The temperature evolution of the environment has a balancing impact on the effective accretion rates. If the accretion rate is high, the atoms are rapidly depleted from the gas, which then leads to a lower sublimation temperature and more desorption, until the temperature further cools down.

4. Conclusion

This study is unique because: (a) we have, for the first time, explored the variation in the efficiency of sticking for different atoms and molecules on an amorphous carbonaceous dust grain; (b) we have studied the dynamics of grain accretion from the gas-phase over a wide temperature range, applicable to astrophysical environments in which carbonaceous dust nucleation is expected to occur, namely the ejecta of supernovae and AGB stars; (c) we have developed the necessary tools to quantify the rate of grain growth through accretion of gas-phase species on a dust surface. This study is particularly important for cases where dust seeds are synthesized from gas-phase clusters, while the molecule and dust formation occur simultaneously. The abundances of the species which can stick on the surface therefore can be complemented by chemical reactions and sticking rates. We chose here to limit the accuracy of the sticking coefficients to 10^{-3}, as the calculations would be too computationally expensive to reach a higher accuracy (10 times more collisions are necessary to compute sticking coefficients with an accuracy of 10^{-4}). This therefore limits this study to the most abundant species found in the media of interest, as the gas species with relative abundances to the main species of 10^{-4} or lower will

have a contribution at the limit of the sensitivity of our model. This is not a problem as the most abundant species will be those contributing to the growth of carbonaceous dust.

We found that atoms such as H, O, and C have sticking probabilities on a carbonaceous dust grain that range between 0.1 and 0.75. In contrast, H_2 and CO molecules have an almost negligible probability of sticking to dust grains. Dust formation in stellar winds occurs concurrently with gas-phase nucleation processes (Cherchneff & Cau 1999; Sarangi et al. 2018). The specific abundances of carbon, oxygen, and hydrogen vary from star to star and between supernovae. In addition, the physical conditions, mainly the gas temperature and densities, define the relative efficiency between routes of dust production and molecular formation. In environments where carbon dust forms, most of the O atoms are locked up in CO molecules. Moreover, the gas temperature at which CO molecules may form is much higher than the sublimation temperature of carbonaceous dust (Sarangi et al. 2018). Hence, in a cooling gas, before the smallest carbon dust grains are formed, all the O atoms are depleted. In this study, we show that even though O atoms have a high sticking efficiency, the sticking efficiency of CO molecules is nearly zero. So amorphous carbon dust grains are not expected to accrete O atoms on their surfaces in these environments, neither in atomic, nor in molecular form.

Grain growth through accretion of C and H atoms depends on the number of available atoms in the gas, after the smallest dust grains or dust-seeds are formed. Chemical modeling (Sarangi et al. 2018) suggests that C atoms often tend to form small clusters of C-chains in the gas-phase. Based on the present results on the sticking of H_2 and CO, we find it unlikely that small molecules with saturated valences are efficient in aiding the grain growth process via accretion on the dust surface.

Our study points out that the difference in effective accretion rates of C and H may shape the structure of a circumstellar or interstellar grain of carbon dust. The strong temperature dependence of H-sticking and C-sticking reported in this study, in the future, could help us understand the aromaticity of carbon-dust in the ISM and the routes for PAH condensation (Dartois et al. 2007).

This study will be further extended to silicate-type dust, that is found nearby O-rich stars, for which the dust grain structure is more challenging, and includes various chemical species. It will also be of great interest to the astrophysical modeling community to provide sticking coefficients for conditions where the temperature of the gas and of the dust differ, for both carbonaceous and silicate grains. This is particularly helpful for the interstellar medium and gas clouds, where the dust temperature remains low, while incident species can have temperatures spanning a large range. This will be considered in future work, where it will be interesting to see which temperature, namely, that of the dust or the gas, has a greater influence on the sticking process.

References

Al-Halabi, A., van Dishoeck, E. F., & Kroes, G. J. 2004, J. Chem. Phys., 120, 3358
Andersen, A., Höfner, S., & Gautschy-Loidl, R. 2003, Proc. Int. Astron. Union, 210, A13
Bocchio, Marco, Jones, Anthony P., & Slavin, Jonathan D. 2014, A&A, 570, A32
Buch, V., & Zhang, Q. 1991, ApJ, 379, 647
Cazaux, S., Morisset, S., Spaans, M., & Allouche, A. 2011, A&A, 535, A27
Chaabouni, H., Bergeron, H., Baouche, S., et al. 2012, A&A, 538, A128
Chenoweth, K., van Duin, A. C. T., & Goddard, W. A. 2008, J. Phys. Chem. A, 112, 1040
Cherchneff, I. 2000, in The Carbon Star Phenomenon, 177, ed. R. F. Wing, 331
Cherchneff, I., & Cau, P. 1999, Proc. Int. Astron. Union, 191, 251
Cherchneff, I., Le Teuff, Y. H., Williams, P. M., & Tielens, A. G. G. M. 2000, A&A, 357, 572
Dartois, E., Geballe, T. R., Pino, T., et al. 2007, A&A, 463, 635
Deringer, V. L., & Csányi, G. 2017, Phys. Rev. B, 95, 094203
Deringer, V. L., Caro, M. A., Jana, R., et al. 2018, Chem. Mater., 30, 7438
de Rooij, E. D., Kleyn, A. W., & Goedheer, W. J. 2010, Phys. Chem. Chem. Phys., 12, 14067
Draine, B. T. 2011, Physics of the Interstellar and Intergalactic Medium (Princeton University Press)
Dwek, E., & Cherchneff, I. 2011, ApJ, 727, 63
Dwek, E., & Scalo, J. M. 1980, ApJ, 239, 193
Ehrenfreund, P., & Cami, J. 2010, Cold Spring Harb. Perspect. Biol., 2
Fabbian, D., Nissen, P. E., Asplund, M., Pettini, M., & Akerman, C. 2009, A&A, 500, 1143
Gobrecht, D., Plane, J. M., Bromley, S. T., Decin, L., & Cristallo, S. 2019, Proc. Int. Astron. Union, 15, 245
Henning, T. 2010, ARA&A, 48, 21
Hirashita, H. 2012, MNRAS, 422, 1263
Hirashita, H., & Kuo, T.-M. 2011, MNRAS, 416, 1340
Hollenbach, D., & Salpeter, E. E. 1970, J. Chem. Phys., 53, 79
Hollenbach, D., & Salpeter, E. E. 1971, ApJ, 163, 155
Hoover, W. G. 1985, Phys. Rev. A, 31, 1695
Jones, A. P., & Nuth, J. A. 2011, A&A, 530, A44
Laffon, C., Ferry, D., Grauby, O., & Parent, P. 2021, Nat. Astron., 5, 445
Leitch-Devlin, M. A., & Williams, D. A. 1985, MNRAS, 213, 295
Marchione, D., Rosu-Finsen, A., Taj, S., et al. 2019, ACS Earth Space Chem., 3, 1915
Marini, E., Dell'Agli, F., Groenewegen, M. A. T., et al. 2021, A&A, 647, A69
Masuda, K., & Takahashi, J. 1997, Adv. Space Res., 19, 1019
Nanni, A., Groenewegen, M. A. T., Aringer, B., et al. 2019, MNRAS, 487, 502
Nashimoto, M., Hattori, M., Poidevin, F., & Génova-Santos, R. 2020, ApJ, 900, L40
Nosé, S. 1984, J. Chem. Phys., 81, 511
Oli, B. D., Bhattarai, C., Nepal, B., & Adhikari, N. P. 2013, in Advanced Nanomaterials and Nanotechnology (Springer Berlin Heidelberg), 515
Potapov, A., & McCoustra, M. 2021, Int. Rev. Phys. Chem., 40, 299
Potapov, A., Jäger, C., & Henning, T. 2018, ApJ, 865, 58
Potapov, A., Jäger, C., & Henning, T. 2020, Phys. Rev. Lett., 124, 221103
Sarangi, A. 2022, A&A, 668, A57
Sarangi, A., Matsuura, M., & Micelotta, E. R. 2018, Space Sci. Rev., 214, 63
Stuart, B. H. 2004, Infrared Spectroscopy: Fundamentals and Applications (John Wiley and Sons, Ltd)
Tielens, A. G. G. M. 1998, ApJ, 499, 267
Tielens, A. 2022, Front. Astron. Space Sci., 9
van Duin, A. C. T., Dasgupta, S., Lorant, F., & Goddard, W. A. 2001, J. Phys. Chem. A, 105, 9396
van Duin, A. C. T., Goddard, W. A., Islam, M. M., et al. 2023, ReaxFF 2023.1, SCM, Theoretical Chemistry (Amsterdam, The Netherlands: Vrije Universiteit)
Veeraghattam, V. K., Manrodt, K., Lewis, S. P., & Stancil, P. C. 2014, ApJ, 790, 4
von Keudell, A., Meier, M., & Hopf, C. 2002, Diam. Relat. Mater., 11, 969

Appendix A: Additional table

Table A.1. Sticking coefficient values. Given for physisorption, chemisorption, and estimated chemisorption (asymptotic value) processes for H, H$_2$, C, O, and CO colliding with amorphous carbon.

Collider	Process	Temperature (K)											
		50	100	150	250	500	750	1000	1250	1500	1750	2000	2250
H	Physis.	0.039 ±0.007	0.001 ±0.001	0.000 ±0.000	0.000 ±0.000	0.000 ±0.000	0.000 ±0.000	0.000 ±0.000	0.000 ±0.000	0.000 ±0.000	0.000 ±0.000	0.000 ±0.000	0.000 ±0.000
	Chemis.	0.704 ±0.012	0.559 ±0.015	0.509 ±0.019	0.420 ±0.013	0.362 ±0.014	0.422 ±0.017	0.409 ±0.019	0.384 ±0.024	0.381 ±0.028	0.426 ±0.026	0.431 ±0.018	0.500 ±0.021
	Est. Chemis.	0.742 ±0.019	0.561 ±0.016	0.509 ±0.019	0.420 ±0.013	0.362 ±0.014	0.422 ±0.017	0.409 ±0.019	0.384 ±0.024	0.381 ±0.028	0.426 ±0.026	0.431 ±0.018	0.500 ±0.021
H$_2$	Physis.	0.846 ±0.013	0.518 ±0.014	0.150 ±0.023	0.000 ±0.000	0.000 ±0.000	0.000 ±0.000	0.000 ±0.000					
	Chemis.	0.000 ±0.000	0.000 ±0.000	0.003 ±0.002	0.000 ±0.000	0.004 ±0.002	0.001 ±0.001	0.000 ±0.000					
C	Physis.	0.489 ±0.018	0.214 ±0.018	0.019 ±0.006	0.000 ±0.000	0.000 ±0.000	0.000 ±0.000	0.000 ±0.000	0.000 ±0.000	0.000 ±0.000	0.000 ±0.000	0.000 ±0.000	0.000 ±0.000
	Chemis.	0.031 ±0.005	0.074 ±0.009	0.062 ±0.008	0.092 ±0.010	0.166 ±0.008	0.231 ±0.016	0.247 ±0.018	0.295 ±0.016	0.299 ±0.020	0.335 ±0.015	0.347 ±0.013	0.380 ±0.018
	Est. Chemis.	0.276 ±0.005	0.116 ±0.013	0.064 ±0.008	0.092 ±0.010	0.166 ±0.008	0.231 ±0.016	0.247 ±0.018	0.295 ±0.016	0.299 ±0.020	0.335 ±0.015	0.347 ±0.013	0.380 ±0.018
O	Physis.	0.241 ±0.018	0.138 ±0.012	0.020 ±0.005	0.000 ±0.000	0.000 ±0.000	0.000 ±0.000	0.000 ±0.000	0.000 ±0.000	0.000 ±0.000	0.000 ±0.000	0.000 ±0.000	0.000 ±0.000
	Chemis.	0.208 ±0.013	0.305 ±0.020	0.318 ±0.018	0.280 ±0.020	0.236 ±0.013	0.246 ±0.021	0.277 ±0.018	0.272 ±0.015	0.305 ±0.017	0.339 ±0.022	0.331 ±0.012	0.276 ±0.011
	Est. Chemis.	0.389 ±0.027	0.426 ±0.031	0.327 ±0.021	0.280 ±0.020	0.236 ±0.013	0.246 ±0.021	0.277 ±0.018	0.272 ±0.015	0.305 ±0.017	0.339 ±0.022	0.331 ±0.012	0.276 ±0.011
CO	Physis.	0.780 ±0.019	0.658 ±0.014	0.516 ±0.021	0.214 ±0.013	0.014 ±0.004	0.001 ±0.001	0.000					
	Chemis.	0.000 ±0.000	0.000 ±0.000	0.000 ±0.000	0.000 ±0.000	0.000 ±0.000	0.000 ±0.000	0.000 ±0.000					